Novel Aspects of a Convenient Synthesis and of Electroproperties of Derivatives Based on Diphenylamine

by **Krzysztof Idzik**[a]), **Jadwiga Sołoducho***[a]), **Joanna Cabaj**[a]), **Mariusz Mosiądz**[a]), **Mieczysław Łapkowski**[b]), and **Sylwia Golba**[b])

[a]) Wrocław University of Technology, Department of Chemistry, Wybrzeże Wyspiańskiego 27, PL-50-370 Wrocław

[b]) Silesian University of Technology, Department of Chemistry, Strzody 9, PL-44-100 Gliwice

The substituted monomers **4a**,**c**,**d**, **5a**,**b**, **6a**, **7a**,**b**, and **8a** of novel poly(diphenylamines), possessing the respective photochromic groups, were synthesized by the *Stille* cross-coupling methodology (*Scheme*). The hyperbranched structures were characterized by ^{1}H- and ^{13}C-NMR spectroscopy. The obtained monomers show good stability in common organic solvents such as $CHCl_3$, toluene, and CH_2Cl_2, and exhibit excellent thermal stability. Electrochemical results and theoretical calculations suggest that oxidation and reduction of the monomers start from the side of the amine function and the five-membered heterocyclic ring moieties, respectively.

1. Introduction. – Advances in organic electronics have triggered intensive research effort towards the development of efficient materials owing excellent performance and potential applications [1].

Polymers constructed from diphenylamine (DPA) building blocks [2] are versatile materials that exhibit a variety of advanced functional properties such as high hole-transporting and light-emitting efficiencies, large two-photon absorption cross sections, high photorefractivity and photoconductivity, and large stabilization effect on high-spin polyradicals in organic magnets. These materials thus promise an array of technological applications in organic electronics, photonics, and spintronics. The multifaceted functionalities of such materials are partially associated with good co-planarity of the aromatic rings surrounding the central N-atom in the phenylamine unit. The lone-pair electrons on the central N-atom help to enhance the electronic communication along the macromolecular chains and make them to behave as strong electron donors.

Many research groups have worked on the design and synthesis of DPA-based linear polymers. The frontier of polymer research is now moving from the macromolecules with a one-dimensional linear structure to three-dimensional dendritic/hyperbranched structures, with the expectation that the novel molecular architecture of the latter will impact functional properties that are inaccessible by the former [3].

2. Results and Discussion. – 2.1. *Synthesis.* Supplementing our previous publication [4], we now report a systematic investigation on the synthesis and electrochemical and field effects of carriers in a series of new polymer semiconductors based on diphenylamine. The new conjugated monomers **4** – **8** were obtained from commercially available diphenylamine **1** by a multi-step procedure according to the synthetic route

Scheme

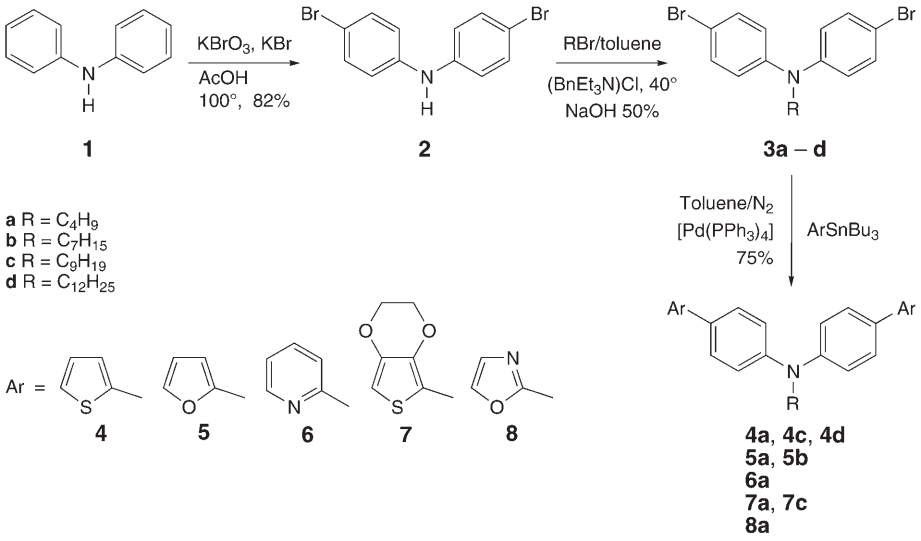

shown in the *Scheme*. Bromination of **1** at the 4-positions was achieved by potassium bromide/potassium bromate in AcOH, which gave bis(4-bromophenyl)amine (**2**). The amino group in **2** was alkylated by RBr in the presence of benzyltriethylammonium chloride ($(BnEt_3N)Cl$) as phase-transfer catalyst to yield the tertiary amines **3a**–**d**. Palladium-catalyzed *Stille* coupling [4] of the amines **3** with tributyl(2-thienyl)-, tributyl(furan-2-yl)-, tributyl(pyridin-2-yl)-, tributyl(2,3-dihydrothieno[3,4-*b*]-1,4-dioxin-5-yl)-, and tributyl(oxazol-2-yl)stannane in toluene gave bis(4-arylphenyl)amine monomers **4a**,**c**,**d**, **5a**,**b**, **6a**, **7a**,**b**, and **8a**. All the monomers were obtained as colorful oils or solids and characterized by spectroscopic methods, from which satisfactory spectral data corresponding to their molecular structures were obtained.

2.2. *Properties of* Langmuir–Blodgett (*LB*) *Films Built from Diphenylamine Derivatives.* Building on our previous experience in the field of surface chemistry, we conducted *LB* experiments. For instance, an *N*-alkylbis[4-(2-thienyl)phenyl]amine **4**, dissolved in an organic solvent ($CHCl_3$), was spread on water. Then the organic layer was deposited by the *LB* technique onto a set of eight interdigital, buried Au-electrodes (200 μm wide and spaced) photolithographically fixed on a thermally coated silicon (SiO_2) substrate. Etching canals in the silicon substrate were then filled by a mixture of gold and trace amounts of tungsten. This configuration provides flat, polished (measured by the interferometric method) electrodes, ready for *LB* deposition. All initially nonmeasured under-water films were deposited at a velocity lower than the draining rate of film of carboxylic acids, *i.e.*, 1.3 mm/min. After deposition, the films were stored in a vacuum desiccator prior to use.

Langmuir monomolecular films of diphenylamine derivative **4c** were spread from the $CHCl_3$ solution on high-purity H_2O at 296 K. *Langmuir–Blodgett* deposition was carried out with a *KSV-5000-LB* system at a surface pressure of *ca.* 20–25 mN/m^2.

The sample processing was carried out at *ca.* 296 K, whereas conductivity was measured at 296, 333, and 358 K.

The transference of the obtained *LB* film was of the *Y*-type in the first deposition and of the *Z*-type in the following ones. The relationship between absorbance and number of layers and the constant transfer ratio during the deposition indicated a constant architecture of the *LB*-film layers. The absorption spectra of the diphenylamine-derivative-deposited films confirm also the formation of homogeneous films in good yield (*Fig. 1*).

Fig. 2 shows typical *I*–*V* curves of fabricated *LB* films at room temperature. The *I*–*V* curves are asymmetric and nonlinear. The forward currents follow approximately an exponential trend. This *I*–*V* behavior is connected with diode-like-type conductivity.

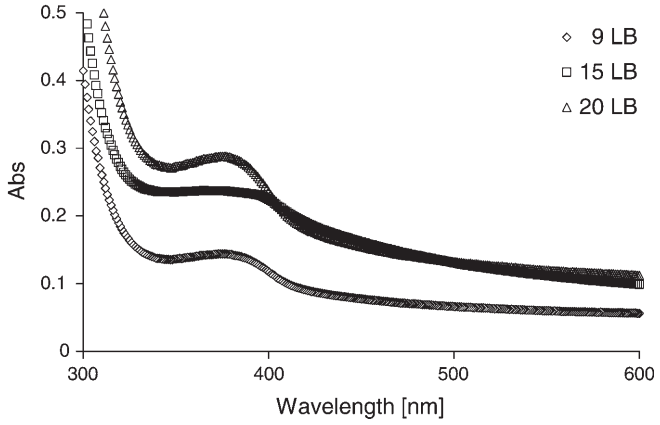

Fig. 1. *Absorption spectra of* LB *films obtained from* N-*nonylbis[4-(2-thienyl)phenyl]amine* (**4c**)*/docosanoic acid* 2 : 1

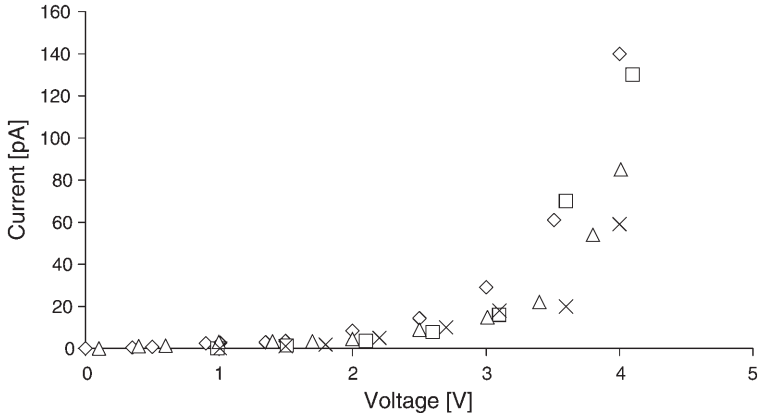

Fig. 2. *Current–voltage characteristics of a 20-layer* LB *film built from* N-*nonylbis[4-(2-thienyl)phenyl]-amine* (**4c**)*/docosanoic acid* 2 : 1. □ = First, △ = second, × = third, and ◇ = fourth cycle.

From current–voltage characteristics obtained at higher temperatures (333 K, 358 K, *Fig. 3*), it was found that the characteristics of the $I-V$ curves become quite linear and symmetrical. The forward currents increased strongly with increasing voltage. At higher temperatures, phenomena of improvement in conjugation of the conducting system are observed. When transient intermolecular charge transfer occurs in a more sustained manner, the character of conductivity is changed and remains linear.

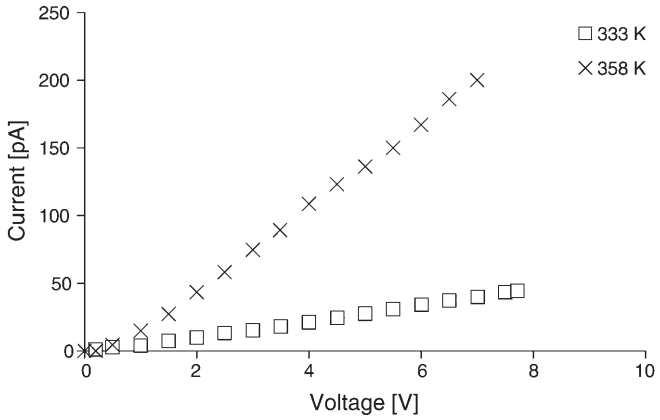

Fig. 3. *Current–voltage characteristics of a 20-layer* LB *film built from* N-*nonylbis[4-(2-thienyl)phenyl]-amine* (**4c**)*/docosanoic acid 2 :1 at different temperatures*

Therefore, these results indicate that the obtained films behave as *p*-type semiconductors. Moreover, good environmental stabilities were observed for the material, what makes it a very promising candidate for sensing elements.

2.3. *Electrochemical Effects of Diphenylamine Derivatives.* Diphenylamine derivatives are able to undergo an oxidative polymerization process according to an established mechanism of electropolymerization [5][6]; the first redox system is attributed to a single-electron oxidation to a radical cation, and the second one leads to a dication (BTFA = **4a**).

$$\mathrm{BTFA} \rightarrow \mathrm{BTFA}^{+} + \mathrm{e}^{-}$$

$$\mathrm{BTFA}^{+} \rightarrow \mathrm{BTFA}^{++} + \mathrm{e}^{-}$$

In the case of a series of methylated oligothiophenes, the first oxidation potential is progressively shifted to more negative values with increasing size of the conjugated backbone, and in addition the oxidation process becomes more and more reversible [7]. In contrast, diphenylamine derivatives of thiophene exhibit reversible oxidation processes, independently of the size of the backbone.

However, the synthesized monomer **4a** is only partially soluble in organic solvents (MeCN) due to its rigid backbone. By gel-permeation chromatography (GPC) against polystyrene standards in THF, the mass-average molecular mass M_w of the polymer pBTFA is determined to be 4900 ($M_n = 2080$, polydispersity near 2.3). The low M_w of

the pBTFA polymer is associated with its poor solubility in organic solvents, and only the THF-soluble fraction was characterized.

The thermal properties of the polymer were evaluated by thermogravimetric analysis (TGA). TGA revealed that the onset decomposition temperature of the polymer under N_2 was 390°.

BTFA (**4a**) is oxidized by a three-step process (*Fig. 4*), as revealed by three clear oxidation peaks at 0.4, 0.9, and 1.4 V and three reduction peaks at the potentials 0.18, 0.18, and 0.33 V. All oxidation processes are reversible. When the oxidation process is ranged to the first oxidation peak, the value of the reduction peak is placed at the potential 0.18 V. In this case, the compound is not electropolymerized, but when the potential increases included the second oxidation peak, we could observe the growing of electroactive yellow layers on the electrode (*Fig. 5*). The polymer obtained from **4a** did not show a reduction wave in the range 0 to -3.0 V which suggests that this polymer is an intrinsic *p*-type semiconductor.

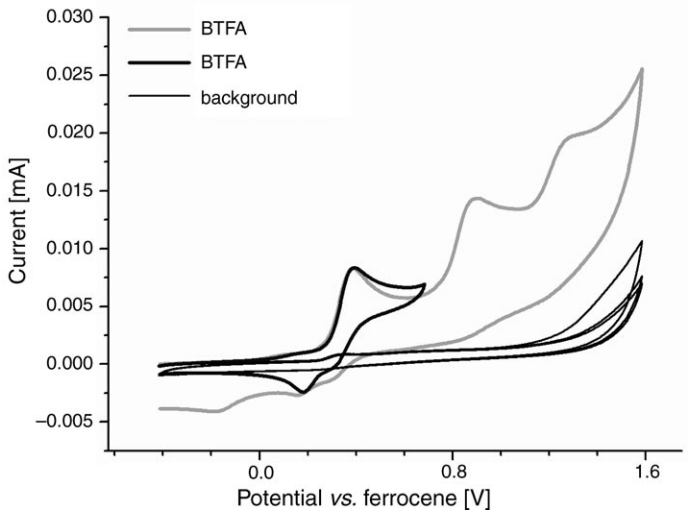

Fig. 4. *Cyclic voltammetry of* N-*butylbis[4-(2-thienyl)phenyl]amine* (= BTFA; **4a**) *in 0.3 mM solution of 0.1M* $(Bu_4N)BF_4$ *in MeCN.* Potential sweep rate $v = 50$ mV/s.

In the case of **5a** (= BFFA), we observed a multistep oxidative process (*Fig. 6*). We found two main, clear oxidation peaks at 0.3 and 1.1 V and one reduction peak at 0.08 V. The entire oxidative process is irreversible. The compound polymerizes near the potential associated with the first oxidation peak, and gave a yellow electroactive film (*Fig. 7*). Similarly to **4a**, the obtained polymer is probably of low molecular mass M_w for the reason given above.

Furthermore, future synthetic modifications will allow to produce unique soluble hybrid polymers that display the same range of tenability. The application of such copolymers to dynamic electrochromic devices, both large and small, will be an important and compelling advancement in the field of electrochromic and conducting heterocyclic polymers.

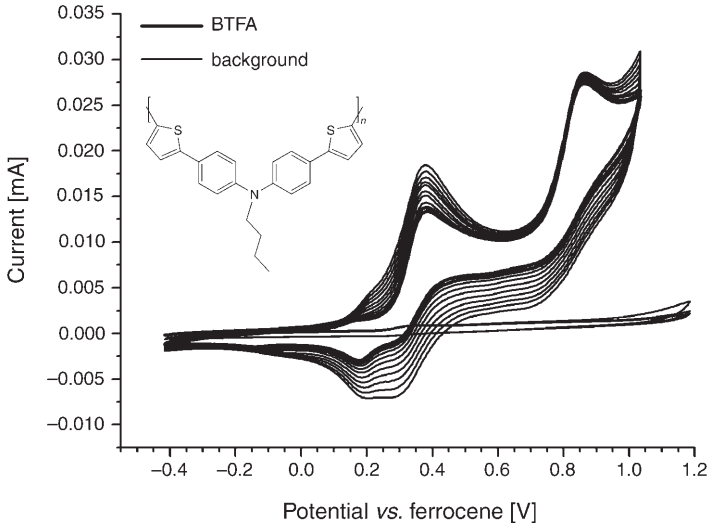

Fig. 5. *Cyclic voltammetry of a poly(BTFA) film in 0.1*M *solution of* $(Bu_4N)BF_4$ *in MeCN.* Potential sweep rate $v = 50$ mV/s.

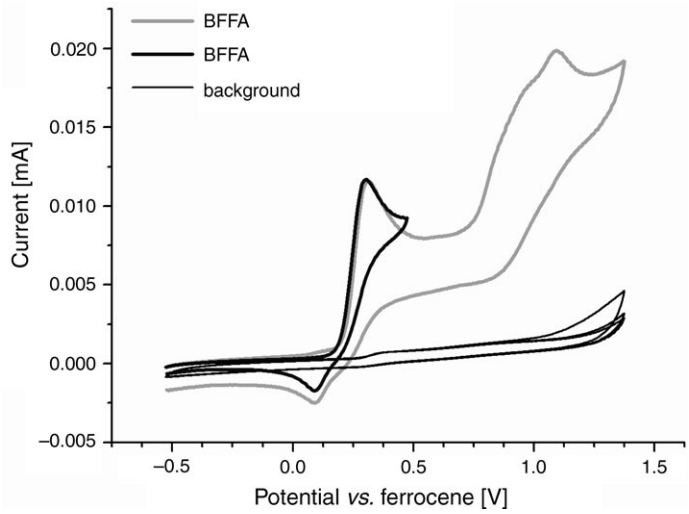

Fig. 6. *Cyclic voltammetry of* N-*butylbis[4-(furan-2-yl)phenyl]amine* (= BFFA; **5a**) *in 0.3 m*M *solution of 0.1*M $(Bu_4N)BF_4$ *in MeCN.* Potential sweep rate $v = 50$ mV/s.

2.4. *Theoretical Study of the Geometry of Diphenylamine Derivatives.* DPA derivatives have an almost planar structure which determines the luminescence characteristics. From our previous experience and theoretical calculations [8], we know that the amine group is able to give a salt with a tetrahedric structure of the N-atom, thus initiating the electropolymerization (see *2.3.*).

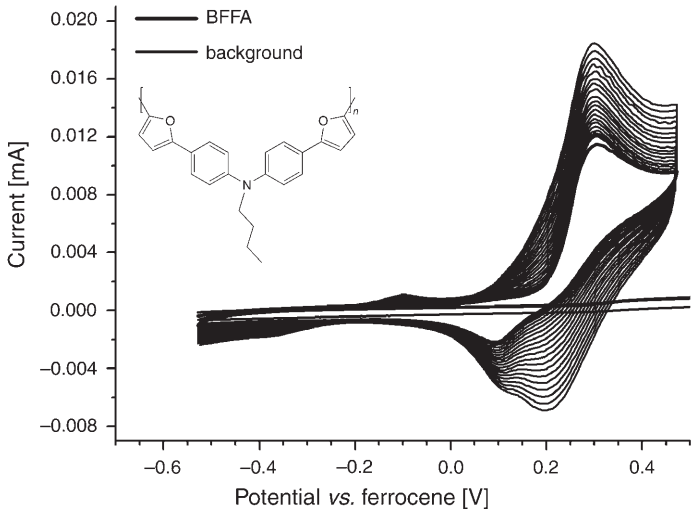

Fig. 7. *Cyclic voltammetry of a poly(BFFA) film in 0.1*M *solution of* $(Bu_4N)BF_4$ *in MeCN.* Potential sweep rate $v = 50$ mV/s.

In the calculated structure of a dimer moiety of **4a**, we found blocked transient intermolecular charge transfer (ICT) due to a blocked conjugation (*Fig. 8*). This phenomenon is illustrated by the HOMO–LUMO visualization (*Fig. 9*). With increasing temperature, continuous conjugation and better conductivity is possible.

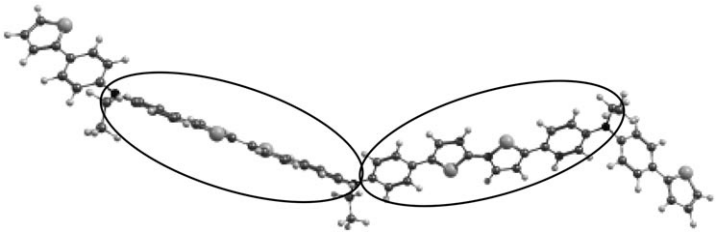

Fig. 8. *Calculated structure of a dimer moiety of* N-*butylbis[4-(2-thienyl)phenyl]amine* (**4a**)

The theoretical study established clear structure–property relationships of the DPA polymers, *i.e.*, the desired electrochemical properties are correlated to the decreasing number of monomer units in the polymer.

3. Conclusions. – In continuation of our previous studies [4][9][10], we performed the efficient synthesis of the novel series of substituted diphenylamine derivatives **4**–**8**, and investigated their functional properties in view of their use as building blocks for electrochemical processing and surface electrochemistry (*LB* films). Thus, Pd-catalyzed *Stille* cross coupling yielded a series of thiophene, furan, pyridine, thienodioxine, and oxazole derivatives **4**–**8** of DPA in 60–90% yield.

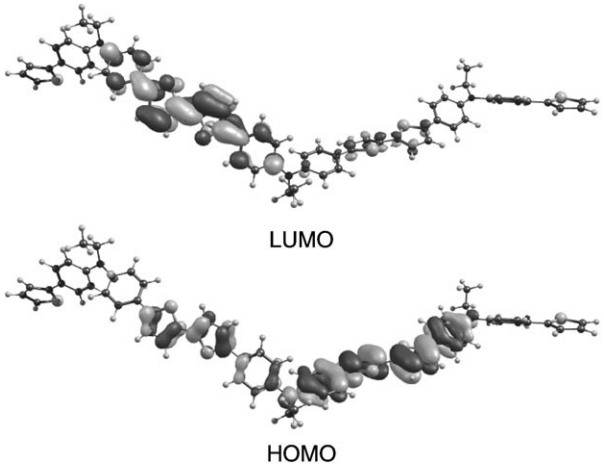

Fig. 9. *HOMO–LUMO visualization of* N-*butylbis[4-(2-thienyl)phenyl]amine* (**4a**)

It should be pointed out that to achieve the improved functional properties of the described materials, it is of great importance to incorporate the electron-donating diphenylamine moiety as a central core in the monomer units. We believe that materials obtained from DPA derivatives may lead to a further increase of the field-effect mobility and thus make these materials attractive for applications in organic sensors, electronic, spintronics, and electrochromic devices [11]. The current strategy is very promising for the application of DPA derivatives as novel building blocks designed for the production of *p*-type semiconductor materials.

Financial support from the Wrocław University of Technology, Grant No 332093, is gratefully acknowledged. We would like to thank also the *Wroclaw Center for Networking and Supercomputing* (*WCSS*) for generous allotment of computer time.

Experimental Part

1. *General. Stille* reactions were performed under N_2. Solvents were carefully dried and distilled from appropriate drying agents prior to use. Commercially available reagents were used without further purification, unless otherwise stated. Monomers **3** were prepared by a standard method [2], and **4**–**8** by the general experimental methodology described in our previous papers (see [4]). Bis(4-bromophenyl)-amine (=4-bromo-*N*-(4-bromophenyl)benzenamine; **2**) was obtained according to a standard method [5]. TLC: *Merck* pre-coated glass plates; visualization with UV light. Flash chromatography (FC): silica gel from *Merck* (230–400 mesh). NMR Spectra: *Bruker-300* spectrometer; $CDCl_3$ solns.; chemical shifts δ rel. to internal $SiMe_4$, J in Hz.

2. *Monomers.* 2.1. N-*Alkylbis(4-bromophenyl)amines* **3a**–**d**. The amines **3a**–**d** were synthesized according to [2] by *N*-alkylation of **2** (3.27 g, 10.0 mmol) with RBr (12.0 mmol) in the presence of $(BnEt_3N)Cl$ (1.0 g, 4.39 mmol) as phase-transfer catalyst in toluene/50% aq. NaOH soln.

N-*Butylbis(4-bromophenyl)amine* (=*4-Bromo*-N-*(4-bromophenyl)*-N-*butylbenzenamine*; **3a**): White microcrystals (3.45 g, 90%). M.p. 61–62°. ^{1}H-NMR ($CDCl_3$): 7.37 (*d*, J = 8.9, 4 H); 6.88 (*d*, J = 8.9, 4 H); 3.65 (*t*, J = 7.7, 2 H); 1.66–1.62 (*m*, 2 H); 1.41–1.30 (*m*, 2 H); 0.96 (*t*, J = 7.3, 3 H). ^{13}C-NMR: 146.7; 132.3; 122.6; 113.9; 52.2; 29.4; 20.3; 14.0. Anal. calc. for $C_{16}H_{17}Br_2N$: C 50.16, H 4.47, N 3.66; found: C 50.46, H 4.40, N 3.71.

N-*Heptylbis(4-bromophenyl)amine* (=*4-Bromo*-N-*(4-bromophenyl)*-N-*heptylbenzenamine*; **3b**): White microcrystals (3.62 g, 85%). M.p. 45–46°. ^{1}H-NMR: 7.32 (*d*, *J* = 8.9, 4 H); 6.82 (*d*, *J* = 8.9, 4 H); 3.59 (*t*, *J* = 7.7, 2 H); 1.61–1.53 (*m*, 2 H); 1.27–1.23 (*m*, 8 H); 0.86 (*t*, *J* = 6.8, 3 H). ^{13}C-NMR: 146.7; 132.2; 122.5; 113.8; 52.4; 31.8; 29.0; 27.2; 26.9; 22.6; 14.0. Anal. calc. for $C_{19}H_{23}Br_2N$: C 53.67, H 5.45, N 3.29; found: C 53.77, H 5.49, N. 3.20.

N-*Nonylbis(4-bromophenyl)amine* (=*4-Bromo*-N-*(4-bromophenyl)*-N-*nonylbenzenamine*; **3c**): Pink microcrystals (3.72 g, 82%). M.p. 30–31°. ^{1}H-NMR: 7.36 (*d*, *J* = 8.9, 4 H); 6.86 (*d*, *J* = 8.9, 4 H); 3.63 (*t*, *J* = 7.7, 2 H); 1.69–1.56 (*m*, 2 H); 1.39–1.21 (*m*, 12 H); 0.90 (*t*, *J* = 6.7, 3 H). ^{13}C-NMR: 146.7; 132.2; 122.5; 113.8; 52.4; 31.8; 29.5; 29.4; 29.2; 27.2; 27.0; 22.7; 14.1. Anal. calc. for $C_{21}H_{27}Br_2N$: C 55.65, H 6.00, N 3.09; found: C 55.56, H 6.11, N 2.99.

N-*Dodecylbis(4-bromophenyl)amine* (=*4-Bromo*-N-*(4-bromophenyl)*-N-*dodecylbenzenamine*; **3d**): Brown oil (3.96 g, 80%). ^{1}H-NMR: 7.35 (*d*, *J* = 8.9, 4 H); 6.86 (*d*, *J* = 8.9, 4 H); 3.62 (*t*, *J* = 7.7, 2 H); 1.69–1.56 (*m*, 2 H); 1.40–1.20 (*m*, 18 H); 0.90 (*t*, *J* = 6.7, 3 H). ^{13}C-NMR: 146.7; 132.2; 122.5; 113.8; 52.4; 31.9; 29.6; 29.5; 29.4; 29.3; 27.3; 27.2; 27.0; 22.7; 14.1. Anal. calc. for $C_{24}H_{33}Br_2N$: C 58.19, H 6.71, N 2.83; found: C 58.21, H 6.76, N 2.86.

2.2. N-*Alkylbis[4-(2-thienyl)phenyl]amines* **4a**,**c**,**d**. According to [4], from **3a**,**c**,**d** (2.0 mmol) and tributyl(2-thienyl)stannane (5.0 mmol).

N-*Butyl-4-(2-thienyl)*-N-*[4-(2-thienyl)phenyl]benzenamine* (**4a**): Green microcrystals (0.70 g, 90%). M.p. 136–137°. ^{1}H-NMR: 7.56 (*d*, *J* = 8.6, 4 H); 7.26–7.24 (*m*, 4 H); 7.10–7.05 (*m*, 6 H); 3.77 (*t*, *J* = 7.7, 2 H); 1.76–1.67 (*m*, 2 H); 1.48–1.39 (*m*, 2 H); 0.99 (*t*, *J* = 7.3, 3 H). ^{13}C-NMR: 147.1; 144.5; 128.0; 127.6; 126.9; 123.8; 122.0; 121.1; 52.1; 29.6; 20.3; 14.0. Anal. calc. for $C_{24}H_{23}NS_2$: C 73.99, H 5.95, N 3.60; found: C 73.91, H 5.90, N 3.57.

N-*Nonyl-4-(2-thienyl)*-N-*[4-(2-thienyl)phenyl]benzenamine* (**4c**): Blue oil (0.75 g, 82%). ^{1}H-NMR: 7.54 (*d*, *J* = 8.7, 4 H); 7.26–7.22 (*m*, 4 H); 7.09–7.03 (*m*, 6 H); 3.74 (*t*, *J* = 7.7, 2 H); 1.85–1.62 (*m*, 2 H); 1.35–1.29 (*m*, 12 H); 0.90 (*t*, *J* = 6.8, 3 H). ^{13}C-NMR: 147.0; 144.4; 127.9; 127.5; 126.9; 123.7; 121.9; 121.0; 52.3; 31.8; 29.6; 29.4; 29.2; 27.4; 27.1; 22.7; 14.1. Anal. calc. for $C_{29}H_{33}NS_2$: C 75.77, H 7.24, N 3.05; found: C 75.40, H 7.33, N 3.16.

N-*Dodecyl-4-(2-thienyl)*-N-*[4-(2-thienyl)phenyl]benzenamine* (**4d**): Blue oil (0.79 g, 79%). ^{1}H-NMR: 7.54 (*d*, *J* = 8.7, 4 H); 7.24–7.22 (*m*, 4 H); 7.10–7.05 (*m*, 6 H); 3.74 (*t*, *J* = 7.7, 2 H); 1.83–1.62 (*m*, 2 H); 1.40–1.26 (*m*, 18 H); 0.89 (*t*, *J* = 6.7, 3 H). ^{13}C-NMR: 146.5; 144.2; 128.2; 128.0; 126.9; 123.9; 122.1; 121.2; 52.8; 31.9; 29.6; 29.6; 29.5; 29.4; 29.3; 27.2; 27.0; 22.7; 14.1. Anal. calc. for $C_{32}H_{39}NS_2$: C 76.59, H 7.83, N 2.79; found: C 76.72, H 7.87, N 2.91.

2.3. N-*Alkylbis[4-(furan-2-yl)phenyl]amine* (**5a**,**b**). According to [4], from **3a**,**b** (2.0 mmol) and tributyl(furan-2-yl)stannane (5.0 mmol).

N-*Butyl-4-(furan-2-yl)*-N-*[4-(furan-2-yl)phenyl]benzenamine* (**5a**): Yellow microcrystals (0.58 g, 82%). M.p. 98–99°. ^{1}H-NMR: 7.60 (*d*, *J* = 8.8, 4 H); 7.46 (*d*, *J* = 1.8, 2 H); 7.06 (*d*, *J* = 8.8, 4 H); 6.55 (*d*, *J* = 3.3, 2 H); 6.48–6.46 (*m*, 2 H); 3.76 (*t*, *J* = 7.7, 2 H); 1.75–1.65 (*m*, 2 H); 1.46–1.37 (*m*, 2 H); 0.97 (*t*, *J* = 7.3, 3 H). ^{13}C-NMR: 154.1; 146.9; 141.4; 124.9; 124.2; 120.9; 111.6; 103.5; 52.1; 29.6; 20.3; 13.9. Anal. calc. for $C_{24}H_{23}NO_2$: C 80.64, H 6.49, N 3.92; found: C 80.54, H 6.56, N 3.98.

4-(Furan-2-yl)-N-*[4-(furan-2-yl)phenyl]*-N-*heptylbenzenamine* (**5b**): Green oil (0.72 g, 90%). ^{1}H-NMR: 7.59 (*d*, *J* = 8.8, 4 H); 7.43 (*dd*, *J* = 1.8, 0.7, 2 H); 7.04 (*d*, *J* = 8.9, 4 H); 6.54 (*dd*, *J* = 3.3, 0.7, 2 H); 6.46–6.45 (*m*, 2 H); 3.73 (*t*, *J* = 7.7, 2 H); 1.72–1.67 (*m*, 2 H); 1.33–1.29 (*m*, 8 H); 0.89 (*t*, *J* = 6.8, 3 H). ^{13}C-NMR: 154.2; 146.9; 141.4; 124.9; 124.2; 120.9; 111.6; 103.5; 52.3; 31.9; 29.1; 27.5; 27.1; 22.6; 14.1. Anal. calc. for $C_{27}H_{29}NO_2$: C 81.17, H 7.32, N 3.51; found: C 81.27, H 7.37, N 3.59.

2.4. N-*Butylbis[4-(pyridin-2-yl)phenyl]amine* (= N-*Butyl-4-(pyridin-2-yl)*-N-*[4-(pyridin-2-yl)phenyl]benzenamine* (**6a**). According to [4], from **3a** (2.0 mmol) and tributyl(pyridin-2-yl)stannane (5.0 mmol): **6a** (0.45 g, 60%). Deep blue oil. ^{1}H-NMR: 8.63–8.61 (*m*, 2 H); 7.93–7.88 (*m*, 4 H); 7.69–7.62 (*m*, 4 H); 7.14–7.09 (*m*, 6 H); 3.77 (*t*, *J* = 7.7, 2 H); 1.70–1.65 (*m*, 2 H); 1.40–1.24 (*m*, 2 H); 0.91 (*t*, *J* = 7.3, 3 H). ^{13}C-NMR: 157.1; 149.5; 148.4; 136.6; 132.2; 127.8; 121.3; 120.9; 119.7; 52.0; 29.6; 20.3; 13.9. Anal. calc. for $C_{26}H_{25}N_3$: C 82.29, H 6.64, N 11.07; found: C 82.59, H 6.69, N 11.00.

2.5. N-*Alkylbis[4-(2,3-dihydrothieno[3,4-*b*]-1,4-dioxin-5-yl)phenyl]amine* (**7a**,**b**). According to [4], from **3a**,**b** (2.0 mmol) and tributyl(2,3-dihydrothieno[3,4-*b*]-1,4-dioxin-5-yl)stannane (5.0 mmol).

N-*Butyl-4-(2,3-dihydrothieno[3,4-*b*]-1,4-dioxin-5-yl)*-N-*[4-(2,3-dihydrothieno[3,4-*b*]-1,4-dioxin-5-yl)phenyl]benzenamine* (**7a**): Blue oil (0.87 g, 86%). ^{1}H-NMR: 7.66 (*d*, *J* = 8.7, 4 H); 7.06 (*d*, *J* = 8.7, 4 H); 6.27 (*s*, 2 H) 4.29 – 4.27 (*m*, 4 H); 4.24 – 4.22 (*m*, 4 H); 3.75 (*t*, *J* = 7.6, 2 H); 1.74 – 1.68 (*m*, 2 H); 1.45 – 1.37 (*m*, 2 H); 0.98 (*t*, *J* = 7.3, 3 H). ^{13}C-NMR: 146.2; 142.3; 137.3; 127.0; 126.3; 120.9; 117.6; 96.5; 64.7; 64.5; 52.1; 29.6; 20.3; 14.0. Anal. calc. for $C_{28}H_{27}NO_4S_2$: C 66.51, H 5.38, N 2.77; found: C 66.55, H 5.42, N 2.79.

*4-(2,3-Dihydrothieno[3,4-*b*]-1,4-dioxin-5-yl)*-N-*[4-(2,3-dihydrothieno[3,4-*b*]-1,4-dioxin-5-yl)phenyl]*-N-*heptylbenzenamine* (**7c**): Blue oil (0.85 g, 74%). ^{1}H-NMR: 7.62 (*d*, *J* = 8.7, 4 H); 7.02 (*d*, *J* = 8.7, 4 H); 4.30 – 4.28 (*m*, 4 H); 4.25 – 4.23 (*m*, 4 H); 3.72 (*t*, *J* = 7.7, 2 H); 1.73 – 1.62 (*m*, 2 H); 1.35 – 1.28 (*m*, 12 H); 0.90 (*t*, *J* = 6.8, 3 H). ^{13}C-NMR: 146.4; 142.4; 137.4; 127.2; 126.3; 121.0; 117.8; 96.6; 64.9; 64.6; 52.5; 32.0; 29.8; 29.6; 29.4; 27.6; 27.4; 22.8; 14.3. Anal. calc. for $C_{33}H_{37}NO_4S_2$: C 68.84, H 6.48, N 2.43; found: C 68.98, H 6.72, N 2.52.

2.6. N-*Butylbis[4-(oxazol-2-yl)phenyl]amine* (= N-*Butyl-4-(oxazol-2-yl)*-N-*[4-(oxazol-2-yl)phenyl]-benzenamine*; **8a**). According to [4], from **3a** (0.77 g, 2.0 mmol) and tributyl(oxazol-2-yl)stannane (1.79 g, 5.0 mmol): **8a** (0.57 g, 80%). Yellow oil. ^{1}H-NMR 7.92 (*d*, *J* = 8.7, 4 H); 7.63 (*d*, *J* = 0.7, 2 H); 7.17 (*d*, *J* = 0.7, 2 H); 7.08 (*d*, *J* = 8.7, 4 H); 3.76 (*t*, *J* = 7.7, 2 H); 1.70 – 1.63 (*m*, 2 H); 1.42 – 1.29 (*m*, 2 H); 0.91 (*t*, *J* = 7.2, 3 H). ^{13}C-NMR: 161.0; 149.0; 138.0; 128.2; 127.6; 120.8; 120.7; 52.0; 29.6; 20.2; 13.9. Anal. calc. for $C_{22}H_{21}N_3O_2$: C 73.52, H 5.89, N 11.69; found: C 73.59, H 5.96, N 11.88.

3. *Oxidative Polymerization*. The electrosyntheses and studies of the polymer films were performed with an *Ecochemie-Autolab* potentiostat/galvanostat, model *PGSTAT20*, driven by a computer. Results were analyzed by the GPES program (general purpose electrochemical system). Cyclic voltammetry (CV) was used for the electrochemical measurements.

The polymer film was synthesized directly on the Pt or ITO (indium tin oxide) electrode, which was used as a working electrode. The Ag-wire served as a pseudoreference electrode, and a Pt-spiral was employed as an auxiliary electrode.

REFERENCES

[1] F. Zhang, M. Jonforsen, D. M. Johansson, M. R. Andersson, O. Inganas, *Synth. Met.* **2003**, *138*, 555.
[2] R. Zheng, M. Haussler, H. Dong, J. W. Y. Lam, B. Z. Tang, *Macromolecules* **2006**, *39*, 7973.
[3] W. Y. Wong, G. J. Zhou, X. M. Yu, H. S. Kwok, Z. Lin, *Adv. Funct. Mater.* **2007**, *17*, 315.
[4] J. Cabaj, K. Idzik, J. Sołoducho, A. Chyla *Tetrahedron* **2006**, *62*, 758.
[5] W. A. Doak, C. Knessl, H. Labaziewicz, S. E. O'Connor, L. Pup, G. Putz, M. Schranz, R. I. Walter, L. Yang, N. H. Werstuik, *Can. J. Chem./Rev. Can. Chim.* **1985**, *63*, 3371.
[6] C. L. Gaupp, J. R. Reynolds, *Macromolecules* **2003**, *36*, 6305.
[7] J. Cremer, C. A. Briehn, *Chem. Mater.* **2007**, *19*, 4155.
[8] J. Doskocz, M. Doskocz, S. Roszak, J. Sołoducho, J. Leszczynski, *J. Phys. Chem. A* **2006**, *110*, 13989.
[9] J. Cabaj, J. Doskocz, J. Sołoducho, A. Chyla, *Heterocycles* **2006**, *68*, 137.
[10] J. Doskocz, J. Sołoducho, J. Cabaj, M. Łapkowski, S. Golba, K. Palewska, *Electroanalysis* **2007**, *19*, 1394.
[11] A. Sapp, G. A. Sotzing, J. R. Reynolds, *Chem. Mater.* **1998**, *10*, 2101.

Received October 25, 2007